Coarsening of precipitation patterns in a moving reaction-diffusion front

A. Volford,[1] I. Lagzi,[2,3] F. Molnár, Jr.,[4] and Z. Rácz[4]

[1]*Department of Physics, University of Technology and Economics, 1521 Budapest, Hungary*
[2]*Department of Meteorology, Eötvös University, 1117 Budapest, Hungary*
[3]*Department of Chemical and Biological Engineering, Northwestern University, Evanston, Illinois 60208, USA*
[4]*Institute for Theoretical Physics–HAS, Eötvös University, 1117 Budapest, Hungary*

Precipitation patterns emerging in a two-dimensional moving front are investigated on the example of NaOH diffusing into a gel containing AlCl$_3$. The time evolution of the precipitate Al(OH)$_3$ can be observed since the precipitate redissolves in the excess outer electrolyte NaOH and thus it exists only in a narrow optically accessible region of the reaction front. The patterns display self-similar coarsening with a characteristic length ξ increasing with time as $\xi(t) \sim \sqrt{t}$. A theory based on the Cahn-Hilliard phase-separation dynamics, including redissolution, is shown to yield agreement with the experiments.

Understanding precipitation patterns formed in a moving reaction front is important both from the basic aspect of extending our knowledge of phase-separation dynamics and from the point of view of technological applications. Indeed, the formation of precipitation structures, well localized in space and time, underlies the notion of the so-called "bottom up" designs [1–4], where one creates structures directly in the bulk. A natural way of realizing such design is to have a reaction-diffusion process and control the dynamics of the reaction zone, i.e., control both the position of the front and the rate of the creation of the reaction product, which yields the precipitate provided its concentration exceeds a threshold value.

Recently, there have been several attempts at controlling reaction zones [3–6] with the most promising results emerging from the use of the ionic nature of the reagents and realizing control through time-dependent electric currents [7]. Although these experiments demonstrate that one can create one-dimensional structures reproducible at the scale of $\sim 500\mu$, the downsizing of the patterns to submicron scales raises several problems related to the front. One of them is the width of the front, which obviously restricts the downscaling in the direction of the motion of the front. The second one is related to the inhomogeneities within the front, which may lead to unwanted precipitation structures in the plane perpendicular to the motion of the front. The scale of these structures clearly limits downscaling in the transverse direction.

The width of reaction fronts has been extensively studied theoretically [8,9], as well as experimentally [10–12], and one has some ideas about the control parameters in this case. Very little is known, however, about the transverse patterns in a moving reaction zone though bulk coarsening has been studied in connection with the so-called gradient-free precipitation experiments [13,14].

Our aim here is to initiate experimental and theoretical studies of the coarsening dynamics of the transverse patterns in reaction zones. This task is made feasible experimentally by overcoming the transparency problem in a way suggested by earlier studies of Liesegang-type phenomena [15–21]. Namely, the reaction-diffusion process is set in a nearly transparent gel and, furthermore, appropriately chosen elec-

trolytes are used so that the reaction product undergoes redissolution in the excess of the outer electrolyte. As a result, precipitate exists only in a narrow region restricted to the reaction zone and its time evolution can be followed in detail.

We observed the patterns in the moving reaction zone in an experimental setup detailed below. The visual observations suggested that the system displayed a self-similar coarsening and this was quantified through the time dependence of the characteristic length scale $\xi(t)$ of the pattern, with the main experimental result being that $\xi(t) \sim \sqrt{t}$. Theoretically, the effective dimensionality of the coarsening system is not entirely obvious, and there are several candidates for driving the coarsening process. We studied this problem by generalizing the Cahn-Hilliard theory of precipitation to include sources and sinks coming from the emergence of the reaction product in the reaction zone and from the redissolution of the precipitate in the excess outer electrolyte, respectively. The numerical solutions of the equations in three dimensions are in agreement with the experimentally observed $\xi(t) \sim \sqrt{t}$. This suggests the natural picture that the sources and sinks are relevant perturbations on the particle conservation, and we observe a curvature-driven late-stage coarsening in a model with nonconserved order parameter [22,23].

In the experiments, a 1 w/wt % agarose (Reanal) gel was prepared with a height of 0.6–0.7 cm in a Petri dish. After the gelation process took place (≈ 2–3 h), the inner electrolyte (AlCl$_3$) was poured on top of the agarose gel to obtain a given concentration in the gel (0.48–0.56 mol/L). After 64 h, the inner electrolyte solution was removed from top of the gel and replaced by the outer electrolyte (NaOH of fixed concentration 2.5 mol/L).

A white precipitation layer formed immediately at the gel interface, and this layer started to move into the gel. The evolution of precipitation pattern in the moving layer was recorded in reflected light using a EOS-20D camera connected to a computer. Typical recording period was $t = 25$ min and we analyzed the processes in this time window supposing that the light intensity is proportional to the precipitation concentration [24].

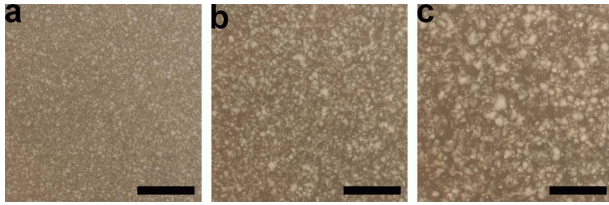As shown in Fig. 1, the patterns have a random appear-

FIG. 1. (Color online) Time evolution of the precipitation pattern in the reaction zone for the samples with [NaOH]=2.5 M (outer electrolyte) and [AlCl$_3$]=0.52 M (inner electrolyte). The front moves perpendicularly to the plane of the picture and the pictures were taken at t_1=180 s (a), t_2=480 s (b), and t_3=960 s (c) after the initiation of the reaction. The length of the scale bars is 1 cm.

ance and they coarsen with time [25]. The coarsening displays self-similarity, as indicated by Fig. 2, where the pictures have been magnified by $1/\sqrt{t}$ with t being the elapsed time from the initiation of the process. The self-similarity can be quantified by measuring the time evolution of the characteristic length $\xi(t)$ of the precipitation structures. We found ξ^2 through calculating the structure factor of the grayscale values of the pattern and evaluating the average of the wave number squared $\xi^2 \sim 1/\langle k^2 \rangle$ [25]. The results for three different inner electrolyte concentrations are displayed in Fig. 3 and we can see a well-defined diffusive growth $\xi^2 \sim 2D_\perp t$ regime.

The transverse diffusion coefficient $D_\perp$ can be estimated from Fig. 3, and we find $D_\perp = \xi^2/2t \approx 5 \times 10^{-10}$ m^2 s^{-1}. It is remarkable that $D_\perp$ is an order of magnitude smaller than the diffusion coefficients of the small hydrated ions.

Our understanding of the observed phenomena is as follows. The hydroxide ion (outer electrolyte) diffuses into the gel, and the white precipitation layer at the gel interface is produced by the reaction with the inner electrolyte (aluminum ions)

$$\text{Al}^{3+}(\text{aq}) + 3\text{OH}^-(\text{aq}) \rightarrow \text{Al(OH)}_3(\text{s}).$$
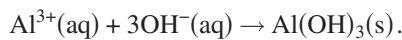
Next, this layer redissolves due to the complex formation of aluminum hydroxide in the excess of hydroxide ions producing a soluble aluminum complex

$$\text{Al(OH)}_3(\text{s}) + \text{OH}^-(\text{aq}) \rightarrow [\text{Al(OH)}_4]^-(\text{aq}).$$
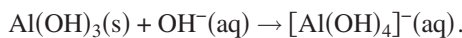
The combination of the precipitation and of the complex-formation processes results in a thin precipitation layer moving through the gel. It should be emphasized, however, that
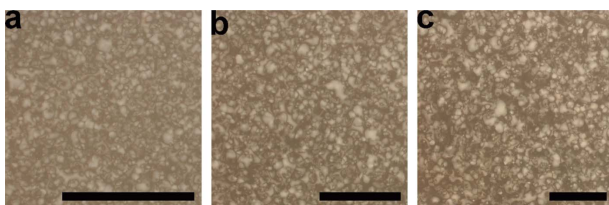

FIG. 2. (Color online) Visual demonstration of the scaling in the evolution seen in Fig. 1. Parts of panels (a) and (b) are magnified by factors $(t_3/t_1)^{1/2}$ and $(t_3/t_2)^{1/2}$, respectively. The scale bars are the same length of 1 cm.
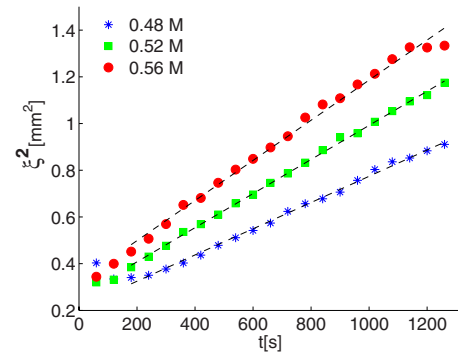

FIG. 3. (Color online) Square of the characteristic length ξ^2 of the precipitation patterns plotted as a function of time t for three inner electrolyte concentrations and at fixed outer electrolyte concentration (a_0=2.5 M). We calculated ξ^2 from the second moment of the structure factor of the patterns.

the motion is solely the transport of chemical species and not of the precipitate.

Within the above picture, the coarsening in the reaction zone emerges from a complicated interplay of the dynamics of the reaction zone, of the aggregation onto the already present precipitate, and of the redissolution process. As a first step in understanding the interplay of these processes, we approached the problem through coarse-grained (mean field) equations by using a model [26] that has been developed in a series of papers during the last decade [7,18].

The three processes we include are as follows. First, the reaction of the electrolytes $A+B \rightarrow C$ yields the reaction product C. Since the process takes place in a gel, no convection is present and it can be modeled as a simple reaction-diffusion process. This reaction provides the source for the precipitation, which is modeled as a phase separation of C's described by the Cahn-Hilliard equation with a source term. Finally, the C's redissolution in the excess A's (complex formation; $A+C \rightarrow$ complex) appears as a sink term both in the Cahn-Hilliard equation and in the reaction-diffusion equation for the A's.

The picture can be further simplified if we assume that $A+B \rightarrow C$ is an irreversible process for totally dissociated electrolytes A and B and that the case of monovalent ions with equal diffusion coefficients are considered. Then the equations take the following form:

$$\partial_t a = D\Delta a - k_1 ab - k_2 ac, \tag{1}$$

$$\partial_t b = D\Delta b - k_1 ab, \tag{2}$$

$$\partial_t c = -\lambda\Delta(\delta f/\delta c) + k_1 ab - k_2 ac + \sqrt{c}\,\eta. \tag{3}$$

Here D is the diffusion coefficient of the ions, while k_1 and k_2 are the rates of reaction and complex formation, respectively. We take k_1 to be large resulting in a reaction zone of negligible width (note that this assumption is compatible with the typical reactions used in experimental setups that result in Liesegang structures). The thermal fluctuations in c are described by a noise term $\sqrt{c}\,\eta$, which conserves the total number of C particles [27]. The free energy (f) underlying
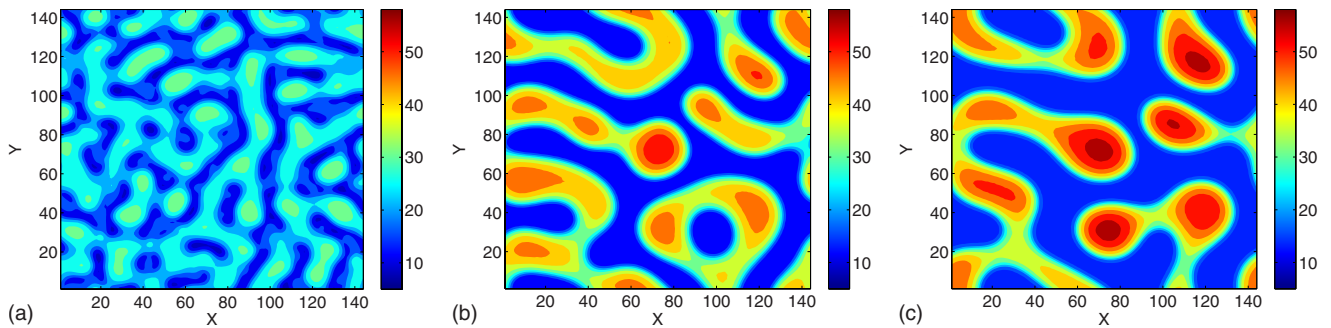
FIG. 4. (Color online) Simulation results for the spatial distribution of C integrated along the z direction. The parameters used were $b_0/a_0 = 0.18$, $c_h/a_0 = 0.2$, $c_l/a_0 = 0$, $D = 10^{-9}$ m^2 s^{-1}, $k_1 = 8.6$ M^{-1} s^{-1}, $k_2 = 0.13$ M^{-1} s^{-1}, $\lambda = 0.83 \times 10^{-9}$ m^2 s^{-1}, $\sigma = 10^{-6}$ m^2, the grid spacing, and the time step were 0.01 mm and 0.003 s, respectively. The snapshots were taken at 75 s, 600 s, and 1200 s.

the thermodynamics of the phase separation (3) is assumed to have minima at some low (c_l) and high (c_h) concentrations, and it is assumed to be of a Ginzburg-Landau form. Its functional derivative most compactly given in terms of a shifted and rescaled concentration $m = (2c - c_h - c_l)/(c_h - c_l)$,

$$\frac{c_h - c_l}{2} \frac{\delta f}{\delta c} = \frac{\delta f}{\delta m} = m - m^3 + \sigma \Delta m. \qquad (4)$$

Finally, σ and λ in Eq. (3) are setting the spatial and the time scales. They can be chosen to reproduce the correct time and length scales in experiments [28].

The initial conditions to the above equations are set according to the experiments. The outer and inner electrolytes are homogeneously distributed in the lower ($z < 0$) and upper ($z > 0$) half spaces with concentrations a_0 and $b_0 \ll a_0$, while the initial concentration of C is $c_0 = 0$ everywhere. For solutions in finite rectangular boxes, we applied no-flux boundary conditions at the borders along the z axis, while periodic boundary conditions were used at the rest of the border planes.

Equations (1)–(3) together with Eq. (4) were discretized on a uniform three-dimensional grid of size $144 \times 144 \times 704$, and finite-size effects were checked on grids of size $160 \times 160 \times 568$ (no effects were observed) and $96 \times 96 \times 1584$ (effects were seen: the final characteristic length was increased roughly by factor of 2).

The resulting ordinary differential equations were integrated in time by Euler method (fast simulations were made feasible by the parallel programming possibilities of video cards [29]). The results from the simulations are summarized in Figs. 4 and 5 [25].

Figure 4 suggests the existence of two stages in the evolution of the system. There is an initial period when the unstable homogeneous density of C's produced by the front begins to evolve toward the equilibrium densities [panel (a) in Fig. 4]. This stage is driven by the initial perturbations (noise), which determines whether the concentration in a given neighborhood grows or diminishes.

The first stage is finished when the high- or low-concentration states are reached in a significant fraction of the system and an initial phase of fast coarsening has also taken already place. The emerging high-concentration regions [panel (b) in Fig. 4] form a structure, which is the base

for the next stage, the self-similar coarsening. It should be noted that the memory of this structure can be recognized throughout the later stages of the coarsening [panel (c) in Fig. 4].

In order to compare with experiments, we calculated the structure factor and the characteristic length $\xi(t)$ by processing pictures as in case of the experiments [25]. The results for various inner electrolyte concentrations are shown in Fig. 5. As we can see, there is a fast initial stage governed by noise and short-scale relaxation to the equilibrium concentrations followed by the late-stage coarsening. The initial large fluctuations in ξ are due to the fact that at the initial stage, there is a significant probability for two precipitation bands to coexist. The averaging of concentration in the z direction yields then an apparent pattern with random correlation length. Since the Cahn-Hilliard equation describes the long-time long-wavelength properties of the coarsening, the short-time fluctuations of ξ may be an artificial feature of the results. Similarly, the explanation of the presence of an induction time in the $b_0 = 0.48$ M experiments may also be outside the scope of the CH description. The late-stage coarsening, however, should be correctly given. $\xi(t)$ is indeed smooth in this regime and, in agreement with the experiments, it shows diffusive behavior ($\xi^2 \sim t$).

We should emphasize that the emergence of a coarsening state is by no means obvious. The rate of the arrival of A and B particles to the front decreases with time (roughly as $a_0/\sqrt{t}$ and $b_0/\sqrt{t}$) and the front can advance only in the presence of surplus As. Thus, it is also a conceivable scenario that due to
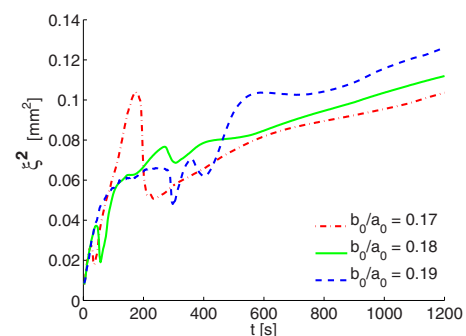

FIG. 5. (Color online) Simulation results demonstrating the diffusive growth $\xi^2 \sim t$ of the characteristic length scale ξ.

the redissolution process ($A+C\rightarrow$ complex), there is only a small concentration of C's in the front with finite (or perhaps even decreasing) correlation length. The selection of a self-similar coarsening state is the result of a delicate interplay between the diffusive advance of the front and the reaction-diffusion-aggregation processes within the front.

In conclusion, we studied the coarsening of precipitation patterns in a thin moving reaction front, and our experiments suggest that the asymptotic dynamics of the system may be interpreted as curvature-driven late-stage coarsening in systems with nonconserved order parameter. The theoretical approach based on the Cahn-Hilliard equation coupled to

reaction-diffusion processes reproduces all relevant findings observed in experiments, but the question of why self-similar coarsening is selected by the dynamics is still to be answered. We believe that, in general, the coupling of reaction fronts with phase-separation processes opens a wide range of possibilities for studying aspects of coarsening and pattern formation and developing this field is of importance for sub-microscopic technological design.

[1] H. K. Henisch, *Periodic Precipitation* (Pergamon Press, New York, 1991).

[2] W. Lu and C. M. Lieber, Nature Mater. **6**, 841 (2007).

[3] I. T. Bensemann, M. Fialkowski, and B. A. Grzybowski, J. Phys. Chem. B **109**, 2774 (2005).

[4] M. I. Lebedeva, D. G. Vlachos, and M. Tsapatsis, Phys. Rev. Lett. **92**, 088301 (2004).

[5] O. Giraldo *et al.*, Nature (London) **405**, 38 (2000).

[6] T. Antal, I. Bena, M. Droz, K. Martens, and Z. Rácz, Phys. Rev. E **76**, 046203 (2007).

[7] I. Bena, M. Droz, I. Lagzi, K. Martens, Z. Rácz, and A. Volford, Phys. Rev. Lett. **101**, 075701 (2008).

[8] L. Gálfi and Z. Rácz, Phys. Rev. A **38**, 3151 (1988).

[9] T. Antal, M. Droz, J. Magnin, Z. Rácz, and M. Zrinyi, J. Chem. Phys. **109**, 9479 (1998).

[10] L. Y.-E. Koo and R. Kopelman, J. Stat. Phys. **65**, 893 (1991).

[11] C. Léger, F. Argoul, and M. Bazant, J. Phys. Chem. B **103**, 5841 (1999).

[12] C. N. Baroud, F. Okkels, L. Ménétrier, and P. Tabeling, Phys. Rev. E **67**, 060104(R) (2003).

[13] S. C. Mueller, S. Kai, and J. Ross, J. Phys. Chem. **86**, 4294 (1982).

[14] S. Kai, S. C. Müller, and J. Ross, J. Phys. Chem. **87**, 806 (1983).

[15] M. Zrínyi, L. Gálfi, E. Smidroczki, Z. Rácz, and F. Horkay, J. Phys. Chem. **95**, 1618 (1991).

[16] R. Sultan and S. Panjarian, Physica D **157**, 241 (2001).

[17] R. Sultan, Phys. Chem. Chem. Phys. **4**, 1253 (2002).

[18] I. Lagzi, P. Pápai, and Z. Rácz, Chem. Phys. Lett. **433**, 286 (2007).

[19] A. Volford, F. Izsák, M. Ripszám, and I. Lagzi, Langmuir **23**, 961 (2007).

[20] B. P. J. D. Costello, Int. J. Unconv. Comput. **4**, 297 (2008).

[21] B. P. J. de Lacy Costello, J. Armstrong, I. Jahan, and N. M. Ratcliffe, Int. J. Nanotechnol. Mole. Comput. **3**, 26 (2009).

[22] K. Binder, Rep. Prog. Phys. **50**, 783 (1987).

[23] A. J. Bray, Adv. Phys. **51**, 481 (2002).

[24] For $t \gg 25$ min, we observed that the coarsening stopped and the pattern froze. This phenomenon (which is not a finite-size effect since it happens irrespective of the gel thickness and the concentration of the inner electrolyte) appears to be rather complex and should be the subject of future studies.

[25] See EPAPS Document No. E-PLEEE8-80-R09911 for (i) evolution of the experimental precipitation pattern in the reaction zone, (ii) calculation of the structure factor, and (iii) evolution of the precipitation pattern in the reaction zone as obtained from the numerical simulation. For more information on EPAPS, see http://www.aip.org/pubservs/epaps.html

[26] T. Antal, M. Droz, J. Magnin, and Z. Rácz, Phys. Rev. Lett. **83**, 2880 (1999).

[27] In numerical solutions, the noise term was realized by exchanging C's at neighboring sites proportionally to $\sqrt{c}\,\eta$, where η is a random number uniformly distributed in the interval $[-0.015, 0.015]$.

[28] Z. Rácz, Physica A **274**, 50 (1999).

[29] The calculations were parallelized with compute unified device architecture (CUDA), the new parallel programming architecture of NVIDIA video cards. A GeForce 8800GTX video card was used to perform computations (2.66 GHz Core2 processor and 4 GB RAM).